Below the first version of the manuscript is presented. The article is published in J. of Electronic Materials, 2014, DOI: 10.1007/s11664-014-3105-6.

Thermoelectric Properties of Tetrathiotetracene Iodide Crystals: Modeling and Experiment

Anatolie CASIAN and Ionel SANDULEAC
Department of Computers, Informatics and Microelectronics,
Technical University of Moldova, Stefan cel Mare av. 168, Chisinau, Rep. of Moldova

A more complete physical model for nanostructured crystals of tetrathiotetracene-iodide that takes into account the interaction of carriers with the neighboring one-dimensional (1D) conductive chains and also the scattering on impurities and defects is presented. For simplicity the 2D approximation is applied. It is shown that this model describes very well the temperature dependencies of electrical conductivity in the temperature interval between 180 and 300 K and of Seebeck coefficient between 50 and 300 K, the highest temperature for which the measurements were reported. For lower temperatures it is needed to also consider the fluctuations of dielectric phase which appear before the metal-dielectric transition. It is found that the predictions made in 1D approximation are valid, if the crystal purity is not very high, the electrical conductivity is limited up to ~ 3.5×10^6 $\Omega^{-1}m^{-1}$ and the thermoelectric figure of merit up to $ZT \sim 4$.

Key words: Thermoelectric, organic crystal, tetrathiotetracene-iodide, Seebeck coefficient, thermal conductivity, thermoelectric figure of merit.

INTRODUCTION

Organic materials attract more and more attention for thermoelectric applications as materials with much more diverse properties and less expensive in comparison with the known inorganic ones. Besides, organic materials usually have a very low thermal conductivity that is favorable for the improvement of thermoelectric efficiency. In poly(3,4-ethylenedioxy-thiophene) (PEDOT) a value of the thermoelectric figure of merit $ZT = 0.25$ has been measured [1] and $ZT \sim 1$ is predicted in this class of materials [2]. Reported in [1] data were analyzed in [3] and it was shown that the increase in the power factor in PEDOT is due mainly to the increase of ionized impurity scattering over the lattice scattering, leading to the increase of the thermopower. The peak power factor occurs for carrier density of $\sim 1 \times 10^{26}$ m^{-3} higher than in inorganic thermoelectric materials and mobility of $\sim 5 \times 10^{-4}$ m^2/V s. ZT was also enhanced due to low thermal conductivity of PEDOT ~ 0.37 W/m K. By minimizing the total dopant volume and increasing the ionization fraction, $ZT = 0.42$ at room temperature was achieved [4] in PEDOT:PSS.

Both *n*-type and *p*-type organic thermoelectric materials with ZT values of 0.1 to 0.2 around 400 K were developed in [5]. A thermoelectric module containing 35 *n-p* single couples was fabricated which demonstrates an output power of 750 μW, the highest for organic materials reported to this date. Prospects for polymer-based thermoelectric materials are discussed in [6].

The iodine-doped pentacene thin films can be potential candidates for good organic thermoelectric materials [7]. It is expected that the nanocomposite approach of organic and inorganic components could create new efficient thermoelectric materials [8-10]. And really, the highest value of $ZT = 0.57$ at room temperature was measured in phenyl acetylene-capped silicon nano particles [11]. This result is obtained due to relatively high Seebeck coefficient $S = 3.2\times10^3$ μV/K and very low thermal conductivity $\kappa = 0.1$ $Wm^{-1}K^{-1}$. For the description of thermoelectric transport in organic materials different theoretical models have been developed [12-15].

The quasi-one-dimensional (Q1D) organic crystals attract special attention. Such crystals join together the thermoelectric advantages of multi component systems with more diverse internal interactions and of low dimensional ones with increased electronic density of states. In molecular nanowires of conducting polymers values of $ZT \sim 15$ and of thermoelectric power factor ~ 500 μW/cm·K at room temperature were predicted [16]. Such predictions are very important, because in this paper the charge and energy transport is described in the hopping model which is applicable in the case of polymers, but usually gives smaller mobility than the band model.

Still higher values of ZT were predicted by us in Q1D charge transfer organic crystals, if the crystal purity is sufficiently high [17]. However, the above predictions were made on the base of a simplified strictly one-dimensional crystal model. From experimental data it is known that in Q1D crystals the electrical conductivity σ along the molecular chains is almost by three orders of magnitude higher than in the direction transversal to chains. Although from this fact it follows that the interaction between the conductive molecular chains is weak, it is absolutely necessary to estimate the effect of interchain interaction and the restrictions on thermoelectric efficiency that this interaction involves.

The aim of the paper is to present a more complete physical model for highly conducting organic nanostructured crystals of tetrathiotetracene-iodide, TTT_2I_3, as thermoelectric material. The carrier interaction with the neighboring 1D conductive chains and also the scattering on neutral impurity and thermally activated structural defects are taken into account. The model becomes rather cumbersome, therefore for simplicity the 2D approximation is applied. It is shown that the

predictions made in 1D approximation are valid only, if the crystal purity is not very high and σ is limited to ~ 3.5×10^6 $\Omega^{-1}m^{-1}$ and $ZT \sim 4$. In this case the scattering on impurities already limits the carriers' mobility. If the crystal purity is higher and, respectively, σ achieves higher values than the ones mentioned above, it is necessary to take into account the interchain interaction, because this interaction begins to limit the carriers' mobility.

TTT_2I_3 CRYSTALS IN 2D APROXIMATION

The structure of Q1D organic crystals of tetrathiotetracene–iodide, TTT_2I_3, has been briefly described in [18]. The crystals have needle shape and are formed of segregate stacks or chains of planar TTT molecules and I_3^- ions. Only TTT chains are conductive, due to large overlap of TTT π-orbitals along the chains. The overlap of orbitals between neighboring TTT chains is very small. Therefore the conduction mechanism along TTT chains is band-like and between the chains is of hopping type. Respectively, the electrical conductivity along the molecular chains is almost by three orders of magnitude higher than in the transversal direction to the chains. Due to this fact, earlier [17-18] we have neglected the possibility for a carrier to pass from one conducting chain to another and have considered the transport in a 1D conduction band. Now we will estimate the effect of interchain interaction and the restrictions on thermoelectric efficiency that this interaction will involve.

TTT_2I_3 crystal is of mixed-valence: two molecules of TTT give one electron to the iodine chain and the carriers are holes. The crystals admit nonstoichiometric composition of the form $TTT_2I_{3\pm\delta}$ with the surplus or deficiency of iodine. Therefore the hole concentration depends on the iodine content and may be higher or lower than the stoichiometric concentration $n = 1.2\times10^{21}$ cm^{-3}. This is very important because usually in order to achieve maximum values for ZT it is needed to optimize the carrier concentration.

The charge and energy transport is described in the tight binding and nearest neighbors' approximations. In this case the energy of the hole with the 2D quasi-wave vector $\boldsymbol{k}$ and projections (k_x, k_y) has the form

$$\varepsilon(\boldsymbol{k}) = -2w_1[1-\cos(k_x b)] - 2w_2[1-\cos(k_y a)], \quad (1)$$

where w_1 and w_2 are the hole transfer energies between the nearest molecules along and between the chains, b and a are lattice constants along and in transversal direction to the chains. The axis x is directed along $\boldsymbol{b}$, and y is in perpendicular direction. The energy in Eq. 1 is measured from the upper margin of the conduction band. The condition of quasi-one-dimensionality requires that w_2 be much less than w_1. In TTT_2I_3 w_2 is $\sim 0.01\, w_1$.

The frequency of longitudinal acoustic phonons is taken in the form

$$\omega_q^2 = \omega_1^2 \sin^2(q_x b/2) + \omega_2^2 \sin^2(q_y a/2), \quad (2)$$

where 2D quasi-wave vector $\boldsymbol{q}$ has the projections (q_x, q_y), and ω_1 and ω_2 are the limit frequencies in the x and y directions, and ω_2 is much less than ω_1.

As in the 1D approximation considered earlier, two of the most important hole-phonon interactions are taken into account, completed by interchain transitions of holes. The first interaction is determined by the fluctuations of polarization energies of molecules surrounding the conduction hole and is similar to that of the polaron. The coupling constant of this interaction is proportional to the mean polarizability of molecule α_0. The second interaction is determined by the fluctuations of transfer energies of the hole between nearest molecules and is similar to that of the deformation potential. Two coupling constants of this mechanism are proportional to the derivatives w_1' and w_2' with respect to the intermolecular distance of w_1 and w_2. The square of matrix element module of hole-phonon interaction has the form

$$\begin{aligned}\left|A(\boldsymbol{k},\boldsymbol{q})\right|^2 = 2\hbar/(NM\omega_q)\{w_1'^2[\sin(k_x b) - \\ \sin((k_x - q_x)b) + \gamma_1 \sin(q_x b)]^2 + \\ + w_2'^2[\sin(k_y a) - \sin((k_y - q_y)a) + \gamma_2 \sin(q_y a)]^2\}\end{aligned} \quad (3)$$

Here M is the mass of TTT molecule, N is the number of molecules in the basic region of the crystal, γ_1 and γ_2 indicate the ratios of amplitudes of the first interaction to the second one in the direction of chains and in transversal direction

$$\gamma_1 = 2e^2\alpha_0/(b^5 w_1'), \ \gamma_2 = 2e^2\alpha_0/(a^5 w_2') \quad (4)$$

where e is the carrier charge. For the p-type band considered here w_1 and w_2 are positive and exponentially decrease with the increase of intermolecular distance. Therefore γ_1 and γ_2 will be negative.

The scattering of holes on impurities and thermally activated defects is also taken into account. The impurities and defects are considered point like and neutral. In this case the impurity and defect scattering rates are described by the dimensionless parameters D_0 and $D_1\exp(-E_a/k_0T)$, where E_a is the activation energy of defect formation and k_0 is the Boltzmann constant. The parameters D_0 and D_1 are proportional to impurity and defect concentrations, respectively, and can be made very small, if the crystal purity and perfection are rather high.

THERMOELECTRIC PROPERTIES

Let's consider that a weak electrical field and a weak temperature gradient are applied along conductive chains. Then the linearized kinetic equation takes the form of Boltzmann one. In the scattering processes of a hole for temperatures $T \gg 1$ K we can neglect the phonon energy [19] and also the transversal kinetic energy of the hole, because these energies are much less than the kinetic energy of the hole along the chains. Then the kinetic equation is solved analytically and the electrical conductivity along TTT chains σ_{xx}, the Seebeck coefficient S_{xx}, the electronic thermal conductivity κ_{xx}^e and ZT can be expressed through the transport integrals R_n as follows

$$\sigma_{xx} = \sigma_0 R_0, \ S_{xx} = (k_0/e)(2w_1/k_0T)R_1/R_2, \quad (5)$$

$$\kappa_{xx}^e = [4w_1^2\sigma_0/(e^2T)](R_2 - R_1^2/R_0), \quad (6)$$

$$ZT = \sigma_{xx} S_{xx}^2 T/(\kappa_{xx}^L + \kappa_{xx}^e), \quad (7)$$

where

$$\sigma_0 = \frac{2e^2 M v_{s1}^2 w_1^3 r}{\pi^2 \hbar abc (k_0 T_0)^2 w_1'^2} \frac{T_0}{T}, \qquad (8)$$

$$R_n = \int_0^2 d\varepsilon \int_0^\pi d\eta [\varepsilon + d(1-\cos\eta) - (1+d)\varepsilon_F]^n \varepsilon(2-\varepsilon) \times$$
$$\times n_{\varepsilon,\eta}(1-n_{\varepsilon,\eta})[s_0\sqrt{\varepsilon(2-\varepsilon)}cth(s_0 T_0\sqrt{\varepsilon(2-\varepsilon)}/T) \times$$
$$\times \gamma_1^2(\varepsilon-\varepsilon_0)^2 + \frac{d^2}{8\varepsilon(2-\varepsilon)}(1+\gamma_2^2+2\sin^2\eta -$$
$$-2\gamma_2\cos\eta) + D_0 + D_1\exp(-E_a/k_0T)]^{-1}. \qquad (9)$$

Here κ_{xx}^L is the lattice thermal conductivity, r is the number of chains through the transversal section of the unit cell, v_{s1} is the sound velocity along chains, a, b, c are the lattice constants, ε_F is the dimensionless Fermi energy in units of $2w_1$, $\varepsilon_0 = (\gamma_1 - 1)/\gamma_1$ is the dimensionless resonance energy in the same units, $s_0 = \hbar v_{s1}/(ak_0T_0)$, $d = w_2/w_1 = w_2'/w_1'$. In order to compare with the 1D approximation, in Eq. 9 we have introduced a new variable $\varepsilon = (1-\cos(k_x b))$ instead of k_x, where ε has the meaning of dimensionless kinetic energy of a hole along chains in units of $2w_1$, as well as a dimensionless quasi momentum $\eta = k_y a$ instead of k_y, $n_{\varepsilon,\eta}$ is the Fermi distribution function in these new variables. In Eq. 9 the signs of γ_1 and γ_2 were changed, thus, further on, they are positive.

In deduction of Eq. 9 the term proportional to $(bv_{s2}/av_{s1})^2$ which comes from the phonon dispersion law and is much less than unity was neglected, where v_{s2} is the sound velocity in the direction perpendicular to chains. From Eq. 9 it is seen that, if we put d = 0, i.e. the interchain interaction is neglected, the results of the 1D approximation follow. In this case the second term in the denominator of Eq. 9 is equal to zero. It is also seen that if the impurity and defect scattering rates are less than unity, the expression under integral (and the relaxation time) in Eq. 9 has a maximum around $\varepsilon = \varepsilon_0$, when $0 < \varepsilon_0 < 2$. It is a consequence of the mutual compensation of both hole-phonon interactions mentioned above [19]. In the 1D case this maximum is limited by the impurity and defect scattering rates. Since the improvement of ZT is determined by the value of this maximum, it was recommended earlier to reduce the impurity and defect scattering rates, i.e. to increase the crystal purity. In the 2D model this maximum is limited also by interchain scattering and the increase of crystal purity after the limitation imposed by interchain scattering will not give an improved result. Therefore, it is very important to investigate this limitation for ZT.

RESULTS AND DISCUSSION

The electrical conductivity σ_{xx}, the thermopower (Seebeck coefficient) S_{xx}, the electronic thermal conductivity κ_{xx}^e and ZT along the conductive chains in TTT_2I_3 crystals have been calculated numerically after Eqs (3) – (9). The crystal parameters are: $M = 6.5\times10^5 m_e$ (m_e is the mass of the free electron), a =18.35 Å, b = 4.96 Å, c = 18.46 Å, w_1 = 0.16 eV, w_1' = 0.26 eVÅ^{-1}, $v_{s1} = 1.5\times10^3$ m/s, E_F = 0.12 eV, d = 0.01 [20]. In order to fit experimental and theoretical data for σ_{xx} and S_{xx} at room T we have chosen D_0 = 0.01, D_1 = 1.6 and γ_1 = 1.53. A small incommensurability between TTT and iodine chains produces disorder into TTT chains and defects [21], more often with small activation energy $E_a \sim 0.024$ eV. Usually organic crystals have large thermal expansion. The coefficient of thermal expansion β is not known in TTT_2I_3. But in antracene $\beta = 14.5\times10^{-5}$ K^{-1}. This value was taken also for TTT_2I_3. The thermal expansion is considered only in the parameter γ_1, because it contains b^{-5} and its value determines the resonance energy which in its turn determines the thermoelectric properties.

In Fig.1 the experimental data [21] for a TTT_2I_3 crystal with almost stoichiometric hole concentration are represented by rhombs. The measured electrical conductivity σ_{xx} along TTT chains at room temperature is 1.8×10^5 Ω^{-1}m^{-1}. It is seen that with decreasing temperature the electrical conductivity firstly increases, but at values lower than ~100 K a smooth metal-dielectric transition takes place. Calculated data are represented by lines: dashed line is for the 2D model and dotted – for the 1D one (in the 1D case only the Fermi energy was a little diminished by 0.0016 eV in order to have the same hole concentration). It is seen that both lines practically coincide. This means that for crystals with relatively high content of impurity and defects the 1D and 2D models give the same results, because the scattering on impurity and defects already limits the carrier mobility. In this case it is sufficient to apply the simpler 1D approximation. The theory describes very well the temperature dependence of σ_{xx} in the interval from 180 K up to 300 K, the highest T for which measurements were made. For lower temperatures, probably the fluctuations of the dielectric phase appear which lead to a slower increase of σ_{xx} and finally to the metal-dielectric transition. This phenomenon is not considered here.

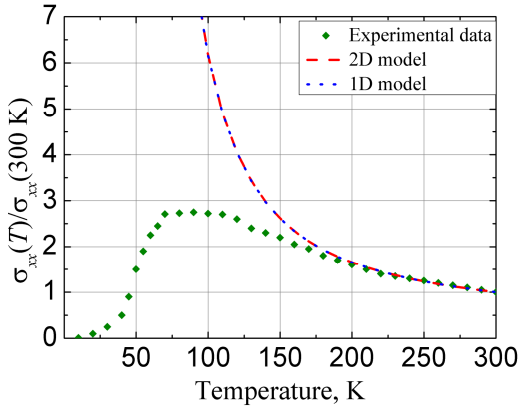

Fig.1. The ratio of electrical conductivity at temperature T to room temperature one: rhombs – experiment; lines – calculations, dashed – for 2D, dotted – for 1D models.

In Fig.2 the data for the thermopower S_{xx} are presented. Since the thermopower is proportional to the ratio R_1/R_0, it is less sensitive to the fluctuations of the

dielectric phase and the theory agrees with the experimental data [22] in a rather large temperature interval. The measurement of thermal conductivity κ_{xx} by direct method has given 1.0 W/Km at room T. Thus, it results $ZT \cong 0.1$, a rather low value.

Crystals with $\sigma_{xx} = 10^6\ \Omega^{-1}m^{-1}$ were also reported [18], however S_{xx} and κ_{xx} were not measured in them. The modeling shows that when σ_{xx} increases, the electronic part of thermal conductivity increases too, so that ZT remains small. But TTT_2I_3 crystals allow nonstoichiometric composition with surplus or deficiency of iodine which is

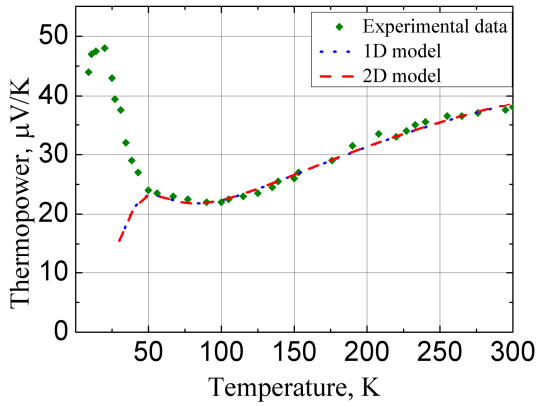

Fig.2. Thermopower as function of temperature: rhombs – experiment; lines – calculations, dashed – for 2D, dotted – for 1D models.

an acceptor and determines the carriers' concentration.

In Fig.3 the dependences of ZT on ε_F at room T are presented. The parameter D now describes the joint rates of scattering on impurity and defects at room T. The lower curves correspond to crystals grown from solution considered in Figs.1 and 2. ZT remains small even in its

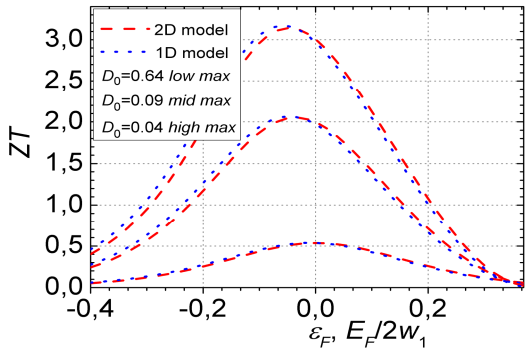

Fig.3. Thermoelectric figure of merit ZT as functions of ε_F for $D_0 = 0.64, 0.09, 0.04$

maximum value. The middle curves correspond to crystals grown by gaseous phase method with $\sigma_{xx} = 10^6\ \Omega^{-1}m^{-1}$. It is seen that if ε_F is diminished down to 0.1 (the hole concentration is diminished from 1.2×10^{21} cm^{-3} up to 0.6×10^{21} cm^{-3}), $ZT \sim 1.4$ is expected. The upper curves correspond to somewhat purer crystals with stoichiometric $\sigma_{xx} = 2\times10^6\ \Omega^{-1}m^{-1}$. In this case $ZT \sim 2$ is predicted for the previous hole concentration. The analysis show that the predictions made in 1D approximation are valid only, if the crystal purity is not very high and σ_{xx} is limited up to ~ $3.5\times10^6\ \Omega^{-1}m^{-1}$ or ZT up to ~ 4. For higher values of σ_{xx}, or respectively of ZT, it is necessary to apply the more complete 2D or even 3D model.

CONCLUSIONS

A more complete physical model for nanostructured crystals of tetrathiotetracene-iodide that takes into account the interaction of carriers with the neighboring one-dimensional (1D) conductive chains and also the carrier scattering on impurities and defects is presented. Modeling of thermoelectric properties have shown: (a) calculated temperature dependences of σ_{xx} and of thermopower S_{xx} for a crystal with electrical conductivity $\sigma_{xx} = 1.8\times10^5\ \Omega^{-1}m^{-1}$ at room temperature coincide very well with the experimental data in the interval 180 - 300K for σ_{xx} and 50 – 300 K for S_{xx}; (b) for this crystal, the calculated temperature dependences of σ_{xx} and of S_{xx} in 1D and 2D approximations practically coincide in the whole temperature interval; (c) the simpler 1D model can be applied for crystals with σ_{xx} limited up to ~ $3.5\times10^6\ \Omega^{-1}m^{-1}$ or $ZT \sim 4$; (d) if the hole concentration is diminished by two times, a value of $ZT \sim 1.4$ is expected in reported stoichiometric crystals with $\sigma_{xx} = 10^6\ \Omega^{-1}m^{-1}$ and $ZT \sim 2$ in those with a somewhat higher $\sigma_{xx} = 2\times10^6\ \Omega^{-1}m^{-1}$.

REFERENCES

1. O. Bubnova, et al., *Nature Materials*, **10**, 429, 2011.
2. R. Yue, *Synt. Met.* 162, 912 (2012).
3. H. L. Kwok, *JEM*, **41**, 476 (2012).
4. G-H. Kim, L. Shao, K. Zhang and K. P. Pipe, *Nat. Matter.* **12**, 719 (2013).
5. Y. Sun , P. Sheng , Dr. C. Di , F. Jiao , Dr. W. Xu , Prof. D. Zhu. *Adv. Mater.*, 2012. DOI: 10.1002/adma.201104305.
6. T. O. Poehler and H. E. Katz. *Energy Environ.* Sci. **5**, 8110 (2012), DOI: 10.1039/C2EE22124A
7. K. Hayashi, Shinano T., Miyazaki Y., and Kajitani T. *J. Appl. Phys.* **109**, 023712 (2011).
8. Y. Y. Wang, K. F. Cai, J. L. Yin, B. J. An, Y. Du, X. Yao. *J Nanopart Res* (2011) 13:533–539. DOI 10.1007/s11051-010-0043-y.
9. W. Q. Ao, L. Wang, J. Q. Li, Fred Pan, C. N. Wu. *JEM*, 40, 2027 (2011).
10. Jihui Yang, Hin-Lap Yip, Alex K.-Y. Jen. *Advanced Energy Materials*, **3**, 549 (2013).
11. Shane P. Ashby, Jorge García-Cañadas, Gao Min & Yimin Chao, *JEM*, **42**, 1495 (2013).
12. G. Kim, K. P. Pipe. *Phys. Rev.* ***B***, **86**, 085208 (2012).
13. J. Chen, D. Wang, Z. Shuai, *J. Chem. Theory Comput.*, **8** (9), 3338 (2012) DOI: 10.1021/ct3004436.
14. Zheyong Fan, Hui-Qiong Wang, and Jin-Cheng Zheng. *J. Appl. Phys.*, **109**, 073713 (2011).
15. D. Wang, L. Tang, M. Long, and Z. Shuai. *J. Phys. Chem. C*, **115** (13), 5940, (2011). DOI: 10.1021/jp108739c.
16. Y. Wang, J. Zhou, and R. Yang. *J. Phys. Chem. C*, 115, 24418 (2011).
17. A. Casian, in: Thermoelectric Handbook, Macro to Nano, Ed. by D. M. Rowe, CRC Press, 2006, Chap.36.
18. A. Casian, J. G. Stockholm, V. Dusciac and V. Nicic, *J. Nanoelectron. Optoelectron.* 4, 95 (2009).

19. A. Casian, V. Dusciac, and Iu. Coropceanu. *Phys. Rev.* ***B*** **66**, 165404 (2002).
20. A. Casian, I. Sanduleac. *J. Nanoelectr. Optoelectron.* 7, 706 (2012).
21. V.F. Kaminskii, M.L. Khidekel', R.B. Lyubovskii and oth. *Phys. Status Solidi* A **44**, 77 (1977).
22. P.M. Chaikin, G. Gruner, I.F. Shchegolev, E.B. Yagubskii. *Sol. State Commun.*, V. 32, 1211 (1979).